An Improved All-Pass Filter Design Using Closed-Form Toeplitz-plus-Hankel Matrix

Yue-Dar Jou[1*] and Fu-Kun Chen[2]

[1]*Department of Electrical Engineering, R. O. C. Military Academy, Feng-Shan Dist., Kaohsiung, 830, Taiwan, R.O.C.*

[2]*Department of Computer Science and Information Engineering, Southern Taiwan University of Science and Technology, Yung-Kang Dist., Tainan, 710, Taiwan, R. O. C.*

Abstract: The least-squares design of infinite impulse response all-pass filter can be formulated as to solve a system of linear equations without directly computing a matrix inversion. The set of linear equations associated matrix is further expressed as a Toeplitz-plus-Hankel matrix such that the optimal filter coefficients are efficiently solved by employing a robust Cholesky decomposition or the split Levinson technique. This paper proposes closed-form expressions for efficiently computing Toeplitz-plus-Hankel matrix based on trigonometric identities. The closed-form expressions of the Toeplitz-plus-Hankel matrix can be directly evaluated as the passband edges are specified without sampling the frequency band as that of the previous computing-efficiency algorithm. The proposed new and simpler closed-form expressions are indicated from simulation results to accurately improve the design performance as well as achieve computational efficiency.

Keywords: All-pass filter, Closed-form, Infinite Impulse Response, Least-squares, Toeplitz-plus-Hankel.

1. INTRODUCTION

Digital infinite impulse response (IIR) all-pass filters exhibit the characteristics of prescribed phase specifications can be preserved without changing magnitude response at all frequencies. These properties enable all-pass filters to find considerable attention in various signal processing applications such as notch filtering, group delay equalizer, phase equalization in communication systems, multi-channel filter banks, construction of wavelet filters, and denoising in ECG signal [1-6]. Much effort has been expended on designing all-pass filters based on the least-squares approximation [7-12] and minimax method [13-15]. The aforementioned approaches [7-15] are generally categorized by solving a set of linear equations, using a linear programming method, applying a second-order cone programming or utilizing a generalized exchange algorithm.

Kidambi [9] presented an efficient and robust weighted least-square method to convert the minimization of nonlinear phase error of the all-pass filter into a quadratic form. The designed all-pass filters results in a least-squares or an equiripple phase error response by selecting a suitable weighting function. Therefore, the filter coefficients are obtained by solving a system of linear equations associated with a Toeplitz-plus-Hankel matrix. Consequently, efficient approaches such as the Cholesky decomposition or the split Levinson technique that requires only $O\left(N^2\right)$ complexity [16] can solve this system of Toeplitz-plus-Hankel associated linear equations. The proposed method in literature [9] is computationally more efficient than conventional method for solving the system of linear equations by directly computing a matrix inversion and multiplication which involves $O\left(N^3\right)$ complexity. Su *et al*. [17, 18] further exploited trigonometric identities and uniformly sampled the frequency band of interest to compute the sum of a series of Toeplitz-plus-Hankel matrix. The improved computing-efficient least-squares algorithm consequently yields the same performance as that of Kidambi's method [9] while markedly reduces the computational requirements.

In this paper, the discrete error phase response of the IIR all-pass filters in [9, 17, 18] is reformulated as an integral square error form [19]. Therefore, the all-pass filter coefficients are obtained by solving a system of linear equations involves a simple and compact Toeplitz-plus-Hankel matrix. The elements of the Toeplitz-puls-Hankel matrix can be explicitly derived when the passband edge frequencies are specified based on trigonometric identities without sampling the band of interest like [17, 18]. The proposed closed-form technique is consequently indicated from simulation results to improve designed performance and preserve computational efficiency as compared to those of methods [17, 18].

*Address correspondence to this author at the Department of Electrical Engineering R.O.C. Military Academy P. O. Box 90602-6 Feng-Shan Dist., Kaohsiung, 830, Taiwan, R.O.C.; Fax: +886-7-7479515;
Email: ydjou@cc.cma.edu.tw

E-ISSN: 2410-2938/14

This remainder of the paper is organized as follows. In Section 2, the least-squares design of IIR all-pass filters is briefly reviewed. In Section 3, the closed-form expressions of the Toeplitz-plus-Hankel matrix using integrals are addressed in detail. In Section 4, the design examples are described to verify the advantages of the proposed method. Section 5 concludes the paper.

2. FORMULATION OF LEAST-SQUARES DESIGN OF IIR ALL-PASS FILTERS

The frequency response of an IIR all-pass filter with *N* real-valued coefficients $a_n, n = 0,\cdots,N-1$, is expressed as

$$A\left(e^{j\omega}\right) = \frac{a_N + a_{N-1}e^{-j\omega} + \cdots + a_0 e^{-j\omega N}}{a_0 + a_1 e^{-j\omega} + \cdots + a_N e^{-j\omega N}} = e^{-j\omega N}\frac{\sum_{n=0}^{N} a_n e^{j\omega n}}{\sum_{n=0}^{N} a_n e^{-j\omega n}} \tag{1}$$

The designed phase response of $A\left(e^{j\omega}\right)$ can be written as

$$\theta(\omega) = -N\omega + 2\tan^{-1}\left(\frac{\sum_{n=0}^{N} a_n \sin(n\omega)}{\sum_{n=0}^{N} a_n \cos(n\omega)}\right). \tag{2}$$

The objective of the IIR all-pass filter design involves in determining the filter coefficient a_n such that the error difference between the designed phase $\theta(\omega)$ and the desired phase $\theta_d(\omega)$ is minimized, that is,

$$e(\omega) = \theta_d(\omega) - \theta(\omega) = \theta_d(\omega) + N\omega - 2\tan^{-1}\left(\frac{\sum_{n=1}^{N} a_n \sin(n\omega)}{1 + \sum_{n=1}^{N} a_n \cos(n\omega)}\right), \tag{3}$$

where $a_0 = 1$ is to avoid trivial filter coefficients. Minimizing the error difference in (3) evidently results in a highly nonlinear optimization and cannot ensure the convergence [9]. Kidambi [9] exploited a phase approximation by assuming that the designed phase response is extremely close to the desired phase, that is, $\theta(\omega) \approx \theta_d(\omega)$ to reduce the complicated design. Consequently, (2) and (3) are approximately expressed as [9, 17, 18]:

$$\tan\left(\frac{\theta(\omega) + N\omega}{2}\right) = \frac{\mathbf{a}^T \mathbf{s}(\omega)}{1 + \mathbf{a}^T \mathbf{c}(\omega)} \approx \frac{\sin\left[\rho_d(\omega)\right]}{\cos\left[\rho_d(\omega)\right]}, \tag{4}$$

where $\rho_d(\omega) = \left(\theta_d(\omega) + N\omega\right)/2$ is an intermediate desired phase. The filter coefficients vector $\mathbf{a}$ and trigonometric functions $\mathbf{c}(\omega), \mathbf{s}(\omega)$ are defined as follows:

$$\mathbf{a} = \begin{bmatrix} a_1 & a_2 & \cdots & a_N \end{bmatrix}^T, \tag{5}$$

$$\mathbf{c}(\omega) = \begin{bmatrix} \cos\omega & \cos(2\omega) & \cdots & \cos(N\omega) \end{bmatrix}^T, \tag{6}$$

$$\mathbf{s}(\omega) = \begin{bmatrix} \sin\omega & \sin(2\omega) & \cdots & \sin(N\omega) \end{bmatrix}^T. \tag{7}$$

Clearly, the tangent function in (4) can be further approximated as a linear equation:

$$\mathbf{a}^T\left[\sin\left[\rho_d(\omega)\right]\mathbf{c}(\omega) - \cos\left[\rho_d(\omega)\right]\mathbf{s}(\omega)\right] \approx -\sin\left[\rho_d(\omega)\right]. \tag{8}$$

The objective function for solving the system of linear equations can be easily formulated as a least-squares error form over the discrete frequency [9, 17, 18]

$$E = \sum_{l=1}^{L}\left\{\mathbf{a}^T \mathbf{s}_1(\omega_l) + \sin\left(\rho_d(\omega_l)\right)\right\}^2, \tag{9}$$

where *L* is the number of frequency sampling points and $\mathbf{s}_1(\omega_l) = \sin\left[\rho_d(\omega_l)\right]\mathbf{c}(\omega_l) - \cos\left[\rho_d(\omega_l)\right]\mathbf{s}(\omega_l)$. Differentiating the objective function in (9) with respect to the filter coefficients and setting $\frac{\partial E}{\partial a_n} = 0$ for $n = 1,2,\cdots N$ results in a system of linear equations $\mathbf{Qa} = \mathbf{d}$, where

$$\mathbf{Q} = \sum_{l=1}^{L} \mathbf{s}_1(\omega_l)\cdot \mathbf{s}_1^T(\omega_l), \tag{10}$$

$$\mathbf{d} = -\sum_{l=1}^{L} \mathbf{s}_1(\omega_l)\sin\left[\rho_d(\omega_l)\right]. \tag{11}$$

The system of linear equations $\mathbf{Qa} = \mathbf{d}$ exists a unique solution $\mathbf{a} = \mathbf{Q}^{-1}\mathbf{d}$ because **Q** is real, symmetric and positive-definite. The conventional least-squares method requires to compute $\mathbf{Q}^{-1}$ which involves $O\left(N^3\right)$ complexity. However, matrix $\mathbf{Q}$ may be ill conditioned when N is large. Solving the system of linear equations can overcome the disadvantage and the matrix inversion is not strictly needed.

3. CLOSED-FORM EXPRESSIONS OF THE TOEPLITZ-PLUS-HANKEL MATRIX

Kidambi [9] has thoroughly demonstrated that the matrix **Q** can be further expanded as the sum of a series of Toeplitz-plus-Hankel matrix. For a $N \times N$ Toeplitz-plus-Hankel matrix, only N and $2N-1$ distinct elements needed to be computed for the Toeplitz and Hankel matrix, respectively. Several iterative and efficient algorithms that involves $O(N^2)$ complexity can solve the Toeplitz-plus-Hankel associated system of linear equations $\mathbf{Qa} = (\mathbf{T}+\mathbf{H})\mathbf{a} = \mathbf{d}$.

In previous works [17, 18], the authors exploited trigonometric identities and sampled the frequency band of interest uniformly to derive the close-form expressions for the Toeplitz-plus-Hankel matrix. Consequently, the closed-form expressions result in the same performance as that of Kidambi's method [9] while substantially reduces the computational complexity. The designed performance and computational complexity are compromised because the closed-form expressions are based on the sampling operation at the frequency band.

The discrete square error in (9) can be modified as an integral form to further improve the designed performance without sampling the frequency band. The objective function is shown as:

$$E' = \int_{\Re} \left\{ \mathbf{a}^T \mathbf{s}_1(\omega) + \sin\left(\rho_d(\omega)\right) \right\}^2 d\omega \,, \tag{12}$$

where $\Re$ is the frequency band of interest. Performing the similar optimization procedure results in the sum of a series of the Toeplitz-plus-Hankel matrix in (10) to be compactly rewritten as:

$$\begin{aligned} Q(i,j) &= \int_{\Re} \sin\left[\rho_d(\omega) - i\omega\right] \sin\left[\rho_d(\omega) - j\omega\right] d\omega \\ &= \frac{1}{2}\left\{ \int_{\Re} \cos(i-j)\omega \, d\omega - \int_{\Re} \cos\left[(i+j)\omega - 2\rho_d(\omega)\right] d\omega \right\} \\ &= T(i,j) + H(i,j). \end{aligned} \tag{13}$$

Therefore, the closed-form expressions of the Toeplitz matrix can be readily classified for the case of $i = j$,

$$T(i,j) = \frac{1}{2}\int_{\omega_{p_1}}^{\omega_{p_2}} \cos\left[0 \cdot \omega\right] d\omega = \frac{\omega_{p_2} - \omega_{p_1}}{2} = \frac{\delta}{2}, \tag{14}$$

where ω_{p_1}, ω_{p_2} are the passband edge frequencies of the IIR all-pass filter and $\delta = \omega_{p_2} - \omega_{p_1}$. Similarly, for the case of $i \neq j$,

$$\begin{aligned} T(i,j) &= \frac{1}{2}\int_{\omega_{p_1}}^{\omega_{p_2}} \cos\left[(i-j)\omega\right] d\omega = \frac{1}{2}\frac{\sin(i-j)\omega}{(i-j)}\Bigg|_{\omega_{p_1}}^{\omega_{p_2}} \\ &= \frac{1}{2}\frac{\sin(i-j)\omega_{p_2} - \sin(i-j)\omega_{p_1}}{(i-j)} \\ &= \frac{\cos\left[(i-j)\Delta/2\right]\sin\left[(i-j)\delta/2\right]}{(i-j)}, \end{aligned} \tag{15}$$

where $\Delta = \omega_{p_1} + \omega_{p_2}$.

However, the elements of Hankel matrix $\mathbf{H}$ and vector $\mathbf{d}$ depend not only on the trigonometric function but also on the intermediate desired phase $\rho_d(\omega)$. Considering for a Hilbert transformer with desired phase response $\theta_d(\omega) = -N\omega - \pi/2$ is designed, the intermediate desired phase yields $\rho_d(\omega) = -\pi/4$. Therefore, the closed-form expressions for the Hankel matrix $\mathbf{H}$ and vector **d** are similarly derived as:

$$\begin{aligned} H(i,j) &= -\frac{1}{2}\int_{\omega_{p1}}^{\omega_{p_2}} \cos\left[(i+j)\omega - 2\rho_d(\omega)\right] d\omega \\ &= -\frac{1}{2}\int_{\omega_{p1}}^{\omega_{p_2}} \cos\left[(i+j)\omega + \frac{\pi}{2}\right] d\omega \\ &= \frac{1}{2}\int_{\omega_{p_1}}^{\omega_{p_2}} \sin\left[(i+j)\omega\right] d\omega = -\frac{1}{2}\frac{\cos(i+j)\omega}{(i+j)}\Bigg|_{\omega_{p_1}}^{\omega_{p_2}} \\ &= \frac{1}{2(i+j)}\left[\cos(i+j)\omega_{p_1} - \cos(i+j)\omega_{p_2}\right] \\ &= \frac{\sin\left[(i+j)\Delta/2\right] \cdot \sin\left[(i+j)\delta/2\right]}{(i+j)} \end{aligned} \tag{16}$$

$$\begin{aligned} d(i) &= -\int_{\omega_{p_1}}^{\omega_{p_2}} \sin\left[\rho_d(\omega)\right] \sin\left[\rho_d(\omega) - i\omega\right] d\omega \\ &= -\frac{1}{2}\int_{\omega_{p_1}}^{\omega_{p_2}} \left\{\cos(i\omega) - \cos\left[i\omega - 2\rho_d(\omega)\right]\right\} d\omega \\ &= -\frac{1}{2}\int_{\omega_{p1}}^{\omega_{p_2}} \cos(i\omega) d\omega - \frac{1}{2}\int_{\omega_{p_1}}^{\omega_{p_2}} \sin(i\omega) d\omega \\ &= -\frac{1}{2}\frac{\sin(i\omega)}{i}\Bigg|_{\omega_{p_1}}^{\omega_{p_2}} + \frac{1}{2}\frac{\cos(i\omega)}{i}\Bigg|_{\omega_{p_1}}^{\omega_{p_2}} \\ &= \frac{\sin(i\omega_{p_1}) - \sin(i\omega_{p_2}) + \cos(i\omega_{p_2}) - \cos(i\omega_{p_1})}{2i} \\ &= -\frac{\cos(i\Delta/2)\sin(i\delta/2)}{i} + \frac{\sin(i\Delta/2)\sin(i\delta/2)}{i} \\ &= -\sqrt{2}\frac{\sin(i\delta/2)\sin(i\Delta/2 + \pi/4)}{i}. \end{aligned} \tag{17}$$

Table 1: Comparison of Computational Requirements for Associated Matrices

<table>
<tr><th rowspan="2" colspan="2">Operation</th><th colspan="4">Algorithm</th></tr>
<tr><th>CONVENTIONAL</th><th>Kidambi [9]</th><th>Su et al. [18]</th><th>Proposed</th></tr>
<tr><td rowspan="3">Q</td><td>+</td><td>$(3L-1)N^2$</td><td></td><td></td><td></td></tr>
<tr><td>*</td><td>$3LN^2$</td><td></td><td></td><td></td></tr>
<tr><td>trig</td><td>$2LN^2$</td><td></td><td></td><td></td></tr>
<tr><td rowspan="3">T</td><td>+</td><td></td><td>$(2L-1)N$</td><td>$3N$</td><td>$3N$</td></tr>
<tr><td>*</td><td></td><td>LN</td><td>$6N$</td><td>$6N$</td></tr>
<tr><td>trig</td><td></td><td>LN</td><td>$3N$</td><td>$2N$</td></tr>
<tr><td rowspan="3">H</td><td>+</td><td></td><td>$(3L-1)(2N-1)$</td><td>$3(2N-1)$</td><td>$3(2N-1)$</td></tr>
<tr><td>*</td><td></td><td>$2L(2N-1)$</td><td>$7(2N-1)$</td><td>$7(2N-1)$</td></tr>
<tr><td>trig</td><td></td><td>$L(2N-1)$</td><td>$3(2N-1)$</td><td>$2(2N-1)$</td></tr>
<tr><td rowspan="3">d</td><td>+</td><td>$(2L-1)N$</td><td>$(2L-1)N$</td><td>$3N$</td><td>$3N$</td></tr>
<tr><td>*</td><td>$2LN$</td><td>$2LN$</td><td>$5N$</td><td>$7N$</td></tr>
<tr><td>trig</td><td>$2LN$</td><td>$2LN$</td><td>$3N$</td><td>$2N$</td></tr>
<tr><td rowspan="3">Total</td><td>+</td><td>$3LN^2-N^2+2LN-N$</td><td>$10LN-3L-4N+1$</td><td>$12N-3$</td><td>$12N-3$</td></tr>
<tr><td>*</td><td>$3LN^2+2LN$</td><td>$L(7N-3)$</td><td>$25N-7$</td><td>$27N-7$</td></tr>
<tr><td>trig</td><td>$2LN^2+2LN$</td><td>$L(5N-1)$</td><td>$12N-3$</td><td>$8N-2$</td></tr>
</table>

+: addition or subtraction operation, *: multiplication or division, trig: sine or cosine operation. In general, $L=4N\sim10N$.

The elements of the Toeplitz-plus-Hankel matrix are observed from these closed-form expressions to associate with the passband edges ω_{p_1} and ω_{p_2}. Only the elements of the first row $T(1,j)$ have to be evaluated for a Toeplitz matrix. However, the elements of the first row $H(1,j)$ and the last row $H(N,j)$ have to be computed for a Hankel matrix. Applying the proposed closed-form expressions to evaluate the Toeplitz-plus-Hankel associated matrices can significantly reduce the computational complexity of the system of linear equations. Table **1** compares the computational requirements for calculating the matrices of $\mathbf{Q},\mathbf{T},\mathbf{H}$ and $\mathbf{d}$ with conventional least-squares and efficient approaches.

The required computational complexity for computing the Toeplitz-plus-Hankel associated matrices in the proposed method and [17, 18], Kidambi method [9], and least-squares approximation is notably $O(N)$, $O(N^2)$, and $O(N^3)$, respectively. The proposed approach derives simple and compact closed-form expressions for calculating the Toeplitz-plus-Hankel matrix based on minimizing the integral square error and exploiting trigonometric identity. In addition, the designed performance can be further improved without sampling the frequency band of interest.

4. SIMULATION RESULTS

MATLAB programming languages are used for designing the IIR all-pass filters that have the same specifications as those of method [18] to illustrate the performance of the proposed technique. The simulations are evaluated on IBM PC with Intel Pentium IV-2.40 and 2.41 GHz duo-core CPU and 1GB RAM.

Example: Design of a Hilbert transformer: For an IIR all-pass filter with length $N=30$, the desired phase response is given by

$$\theta_d(\omega)=-N\omega-\pi/2, \qquad \omega_{p_1}=0.08\pi\le\omega\le\omega_{p_2}=0.92\pi \ . \quad (18)$$

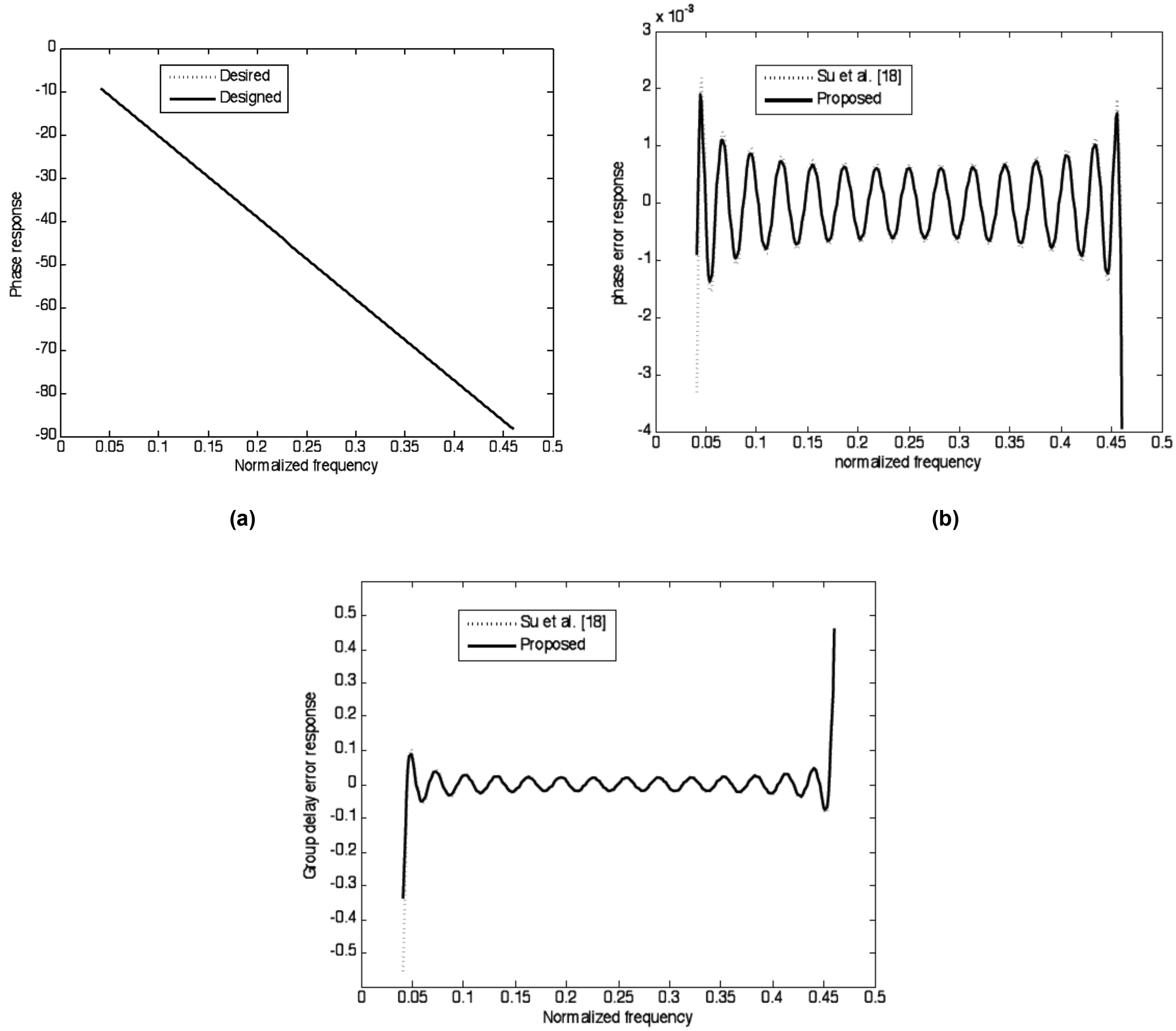

(c)

Figure 1: An 30-th Hilbert transformer. **(a)** Phase response. **(b)** Phase error response. **(c)** Group delay error response.

Using equations (14-17) and the specified passband edge frequencies can explicitly evaluate the closed-form expressions of the Toeplitz-plus-Hankel matrix. Therefore, efficient algorithms such as the Cholesky decomposition or the split Levinson technique can be used to solve the system of linear equations. The designed phase, phase error and group delay error responses are shown in Figure **1**. As seen in Figure **1(a)** and **(b)**, the proposed approach using closed-form Toeplitz-plus-Hankel matrix nearly approximates the desired phase response and achieves smaller peak phase error than that of method [18], respectively. The designed group delay error response is shown in Figure **1 (c)** to extremely close to that designed by the efficient method [18]. The designed results in terms of peak phase error (PPE), mean square phase error (MSPE), peak group delay error (PGDE), mean square group delay error (MSGDE), maximum pole radius (MPR) and CPU time are compared with different techniques. These evaluated values are defined as follows:

$$PPE = \max_{\omega \in \Re} \left| \theta_d(\omega) + N\omega - 2\tan^{-1}\left(\frac{\mathbf{a}^T \mathbf{s}(\omega)}{1 + \mathbf{a}^T \mathbf{c}(\omega)} \right) \right|, \tag{19}$$

$$MSPE = \frac{1}{\pi} \int_{\Re} \left(\theta_d(\omega) + N\omega - 2\tan^{-1}\left(\frac{\mathbf{a}^T \mathbf{s}(\omega)}{1 + \mathbf{a}^T \mathbf{c}(\omega)} \right) \right)^2 d\omega \,, \tag{20}$$

Table 2: Designed Performance Compared With Different Methods.

Algorithm	Least-Squares	Kidambi [9]	Su *et al*. [18]	Proposed
PPE	0.0033 (0.0022)	0.0033 (0.0022)	0.0033 (0.0022)	0.0039 (0.0019)
MSPE	4.713E-5	4.713E-5	4.713E-5	3.868E-5
PGDE	0.5544 (0.2806)	0.5544 (0.2806)	0.5544 (0.2806)	0.4621 (0.2698)
MSGDE	0.2550	0.2550	0.2550	0.1875
MPR	0.9301	0.9301	0.9301	0.9217
CPU time	0.1094	0.1094	0.0313	0.0313

The bracket values in PPE and PGDE represent the peak errors at edge frequencies are excluded.

$$PGDE = \max_{\omega \in \Re} \left| \frac{d\theta_d(\omega)}{d\omega} + N - 2\frac{d}{d\omega}\left\{ \tan^{-1}\left(\frac{\mathbf{a}^T \mathbf{s}(\omega)}{1+\mathbf{a}^T \mathbf{c}(\omega)} \right) \right\} \right|, \quad (21)$$

$$MSGDE = \frac{1}{\pi}\int_{\Re} \left(\frac{d\theta_d(\omega)}{d\omega} + N - 2\frac{d}{d\omega}\left\{ \tan^{-1}\left(\frac{\mathbf{a}^T \mathbf{s}(\omega)}{1+\mathbf{a}^T \mathbf{c}(\omega)} \right) \right\} \right)^2 d\omega \,. \quad (22)$$

The designed performance compared with the methods of least-squares, Kidambi [9], and Su *et al*. [18] is illustrated in Table **2**. The maximum PPE and PGDE values theoretically occur at the band edges. The proposed method yields smaller error responses when the edge frequencies are excluded for comparison. The MSPE and MSGDE values are notably smaller than those of the other methods due to the integral square errors are minimized instead of the discrete summation of errors. Moreover, the MPR designed is 0.9217 which is located inside the unit circle. The designed IIR all-pass filter is consequently not only stable but also efficient to achieve excellent performance. In addition, the stability constraints of the IIR all-pass filter lies in the designed phase $\theta(\omega)$ must be monotonically decreasing and satisfy $\theta(\pi) = \theta(0) - N\pi$ [10]. The designed phase response in the proposed approach is monotonically decreasing and the phase at $\omega = \pi$ is nearly close to $\theta(\pi) = -30\pi$, as indicated in Figure **1(a)**. This constraint also confirms that the proposed closed-form expressions for calculating Toeplitz-plus-Hankel matrix can achieve stable IIR all-pass filters.

A Hilbert transformer with $\omega_{p_1} = 0.08\pi$, $\omega_{p_2} = 0.92\pi$, and varying filter lengths from $N = 32$ to $N = 144$ are designed to illustrate the computational efficiency of the proposed technique. The frequency sampling points is set to $L = 10N$ for least-squares approximation, methods of [9] and [18], whereas the sampling is unnecessary in the proposed method. The CPU time required for computing the optimal all-pass filter coefficients compared with different methods is shown in Figure **2**. Evidently, the proposed closed-form Toeplitz-plus-Hankel matrix grows slowly in the CPU time and retains nearly in constant as the filter length increases. The computational efficiency is slightly superior to that of method [18]. However, the CPU design time of the least-squares method and the efficient method [9] increase rapidly when the filter length is long. Therefore, it is concluded that the proposed closed-form Toeplitz-plus-Hankel matrix has the superiority both in computational efficiency as well as design accuracy.

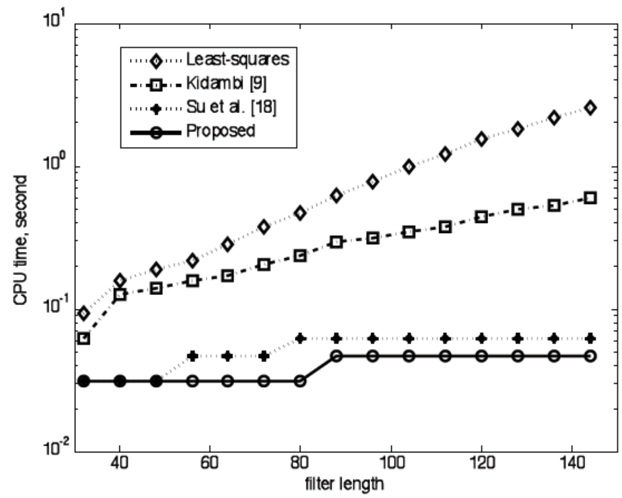

Figure 2: Comparison of CPU time for a Hilbert transformer with varying filter lengths.

5. CONCLUSION

The least-squares design of IIR all-pass filters can be formulated by solving a system of linear equations associated with a Toeplitz-plus-Hankel matrix. Several algorithms that require $O(N^2)$ complexity can efficiently solve the system of linear equations. This paper presents closed-form expressions to simplify the computation of the Toeplitz-plus-Hankel matrix by applying the trigonometric identities and minimizing the integral square errors. As a result, the proposed method not only improves the design accuracy but also reduces the computational requirements.

ACKNOWLEDGMENTS

The authors are grateful to the editor and anonymous reviewers for their valuable recommendations, which truly helped towards an effective presentation of this work. This work was supported by the Ministry of Science and Technology of the Republic of China under the research contracts NSC-100-2221-E-145-005 and MOST-103-2221-E-145-001.

REFERENCES

[1] Regalia PA, Mitra SK, Vaidyanathan PP. The digital all-pass filter: a versatile signal processing building block, Proceedings of the IEEE, 1998; 34: 19-37.

[2] Laakso TI, Valimaki V, Karjalainen M, Laine UK. Splitting the unit delay: tools for fractional delay filter design, IEEE Signal Processing Magazine, 1996; 13: 30-60.

[3] Lang M. All-pass filter design and applications, IEEE Trans Signal Process, 1998; 46: 2505-14.

[4] Regalia PA. A complex adaptive notch filter, IEEE Signal Process Lett, 2010; 17: 937-40.

[5] Stancic G, Nikolic S. Digital linear phase notch filter design based on IIR all-pass filter application, Digit Signal Process, 2013; 23: 1065-9.

[6] Liand W, Zhang YL, Tan JD, Li Y. A novel approache to ECG classification based upon two-layered HMMs in body sensor networks, Sensor 2014; 14: 5994-6011.

[7] Lang M, Laakso TI. Simple and robust method for the design of allpass filters using least-squares phase error criterion, IEEE Trans Circuits and Syst II, Analog and Digit Signal Process, 1994; 41: 40-8.

[8] Chen CK, Lee JH. Design of digital all-pass filters using a weighted least squares approach, IEEE Trans Circuits and Syst II, Analog and Digit Signal Process, 1994; 41: 346-50.

[9] Kidambi SS. Weighted least-squares design of recursive all-pass filters, IEEE Trans Signal Process, 1996; 44: 1553-7.

[10] Tseng CC. Design of IIR digital all-pass filters using least *p*th phase error criterion, IEEE Trans Circuits and Syst II, Analog and Digit Signal Process, 2003; 50:653-6.

[11] Chan SC, Chen HH, Pun CKS. The design of digital all-pass filters using second-order cone programming (SOCP), IEEE Trans Circuits and Syst II, Express Briefs, 2005; 52: 66-70.

[12] Quelhas MF, Petraglia A. Optimum design of group delay equalizers, Digit Signal Process, 2011; 21:1-21.

[13] Ilehara M, Funaishi M, Kuroda H. Design of all-pass networks using Remez algorithm, Proceedings of the IEEE International Symposium on Circuits and Syst, 1991: p. 364-7.

[14] Zhang X, Iwakura H. Design of IIR digital all-pass filters based on eigenvalue problem, IEEE Trans Signal Process, 1999; 47: 554-9.

[15] Lai X, Lin Z. Minimax phase error design of IIR digital filters with prescribed magnitude and phase responses, IEEE Trans on Signal Process, 2012; 60: 980-6.

[16] Sunder S. An efficient weighted least-squares design of linear-phase nonrecursive filters, IEEE Trans Circuits and Syst II, Analog Digit Signal Process, 1995; 42: 359-61.

[17] Su LC, Jou YD, Chen FK. An efficient least-squares design of IIR all-pass filter, in Proceedings of the IEEE TENCON, 2009.

[18] Su, LC, Jou YD, Chen FK. Improved computing-efficiency least-squares algorithm with application to all-pass filter design, Mathematical Problems in Engineering, Article ID 249021, 8 pages, doi: 10.1155/2013/249021, 2013.

[19] Jou YD, Chen FK. Least-squares design of IIR all-pass filters using closed-form toeplitz-plus-hankel matrix, in Proceedings of the IEEE APCCAS, 2014.

Received on 3-8-2014 Accepted on 30-8-2014 Published on 12-1-2015

http://dx.doi.org/10.15379/2410-2938.2014.01.01.03